# Performance indicators and specifications for fusion-bonded-epoxy(FBE)-coated steel rebars in concrete exposed to chlorides

Deepak K. Kamde , Marc Zintel , Sylvia Kessler & Radhakrishna G. Pillai

Published online: 22 Jan 2021.

Submit your article to this journal 

View related articles 

View Crossmark data

Taylor & Francis
Taylor & Francis Group

Check for updates

# Performance indicators and specifications for fusion-bonded-epoxy(FBE)-coated steel rebars in concrete exposed to chlorides

Deepak K. Kamde [a], Marc Zintel[b], Sylvia Kessler [c] and Radhakrishna G. Pillai [a]

aDepartment of Civil Engineering, Indian Institute of Technology Madras, Chennai, India; bConstruction Products at Swiss Steel AG, Emmenbrücke, Switzerland; cConstruction Materials and Building Maintenance Laboratory, Helmut Schmidt University, Hamburg, Germany

## ABSTRACT

Fusion-bonded-epoxy (FBE)-coated steel rebars have been used in many concrete structures in anticipation of better corrosion resistance. However, due to premature corrosion observed, FBE-coated rebars are banned in many parts of the world. On the other hand, such rebars with damaged coating are still used widely in some other parts of the world. This paper discusses the thickness, continuity, flexibility, and chemical composition of coating. Also, the performance indicators such as electrical resistance, UV-resistance, moisture resistance, and chloride diffusion coefficient of coating, and the chloride threshold of FBE-coated rebars are discussed. Laboratory tests adopted techniques (EIS, LA-ICP-MS, and EDX) on samples of coating peeled-off from coated rebars and specimens of coated steel rebars embedded in cement mortar, indicate that more comprehensive and stringent specifications are required to promote the use of quality epoxy materials, FBE-coated steel rebars, and construction practices are recommended.

## 1. Introduction

Corrosion of reinforcement in concrete is one of the major deterioration mechanisms for reinforced concrete (RC) systems. Many RC infrastructure are designed for a corrosion-free service lives of more than 100 years. To achieve such large service lives, Fusion-Bonded-Epoxy (FBE) coated steel rebars are widely used strategy in anticipation of delaying the initiation of corrosion among other available strategies such as use of supplementary cementitious materials, corrosion inhibitors. The mechanisms of prevention of corrosion of steel using FBE coatings are (i) physical barrier or shielding from the surrounding environment (oxygen, moisture, and other deleterious elements), (ii) limiting the formation of anodes and cathodes on steel surface, and (iii) high electrical and ionic resistance making it difficult to form corrosion cells or circuits (Monetta et al., 1993). However, many studies report that the concrete systems with FBE-coated steel rebars experienced major repair due to corrosion within 25 years (Griffith & Laylor, 1999; Pianca et al., 2005; Sagüés et al., 2010b). The premature initiation of corrosion can be attributed to the quality of coating material, application methods, and inadequate construction practices (Sagüés et al., 1991; Sagüés and Zayed, 1991; Sánchez and Sagüés, 2013). ASTM A775-17 is the standard for performance control of FBE-coated steel rebars.

However, the specified performance indicators may not be stringent enough to ensure the service lives of RC systems. Therefore, in the 90s and early 2000s, many countries or states have banned or recommended not to use the FBE-coated steel rebars (Hansson et al., 2000; Pianca et al., 2005; Pyć et al., 2000). However, many developed and developing nations are still using them. Many of these countries are not able to strictly enforce quality control at construction sites. Table 1 provides the details of modifications done in ASTM A775 from 1981 to 2017. However, the recent research in the area of performance of FBE-coated steel rebars indicates that a few of the requirements specified in ASTM A775 may need revision. Concerns associated with a few of these performance indicators are addressed in this paper.

The remainder of this paper is arranged as follows: first, a review on performance indicators of FBE coating and FBE-coated steel rebars is provided. Following this, the experimental program to evaluate the coating characteristics and performance indicators of FBE-coated steel rebars is discussed. Then, results based on existing test methods as per ASTM A775 are presented to evaluate the efficiency of existing specifications. Also, results on the resistance of FBE coating to UV radiation, electrical current, water uptake, and chlorides, and the chloride thresholds of FBE-coated steel rebars to evaluate the service lives are presented. This is followed by

---

**Table 1.** Modifications made in ASTM A775 from 1981 to present.

| Year | Characteristics | Previous specification | Updated specification |
| --- | --- | --- | --- |
| 1981 | | First version of the standard was approved | - |
| 1989 | Allowable damage level | 2% of the coated steel surface area | 1% of the coated steel surface area |
| 1990 | Repair of damage | All damage with area > 64.5 mm$^2$ should be repaired | All the damage should be repaired |
| 1993 | Coating thickness | 90% coating thickness between 5- 12 mil | No single recorded coating thickness measurement shall be less than 80 % of the specified minimum thickness or more than 120 % of the specified maximum thickness |
| 1994 | Bend angle in the flexibility test | 120° | 180° |
| 1995 | Allowable number of holidays | 2 per foot | 1 per foot |
| 1995 | Allowable time gap between sandblasting and coating | 8 hours | 3 hours |
| 1997 | Coating disbondment test | - | Cathodic disbondment test was introduced to ASTM A775 |
| 2004 | Coating thickness limit | 90% coating thickness between 130 to 300 μm (5 - 12 mil) | Coating thickness for rebar size 10 to 16 was changed to 175 to 400 μm (7 to 16 mils). |
| 2007 | Patching materials | - | Specifications for patching material is added to the standard |

recommendations to modify ASTM A775 and other existing guidelines.

## 1.1. Factors affecting the characteristics of epoxy coating

The desired properties of epoxy resin can be achieved by alteration of chemical composition or by controlling the curing time of epoxy coating. For example, mechanical properties such as modulus of elasticity and mechanical strength of FBE coating can be controlled by curing time and suitable dosage of nanomaterials (Cividanes et al., 2014). Also, the desired corrosion resistance can be achieved with thin coating, say a minimum of about 200 μm (Bahadori, 2015; Kobayashi & Takewaka, 1984). The coating thickness of > 420 μm can result in a reduction of the bond between coated steel and concrete (Miller et al., 2003). It was also reported that the coating thickness of < 100 μm can result in many manufacturing defects such as pinholes, discontinuous coating, lower impact resistance and lower flexibility (Kobayashi & Takewaka, 1984; Smith & Virmani, 1996). The pinholes in the coatings can be reduced or eliminated by using additives and fillers. For example, the use of nanoparticles such as $Fe_2O_3$, clay, and carbon black can enhance the packing of epoxy coating (Monetta et al., 1993; Shi et al., 2009). Use of about 1% of clay or $Fe_2O_3$ could enhance the corrosion resistance of steel by providing denser microstructure of the coating and reducing the water penetration through the coating. Whereas, controlled curing and the use of carbon black nanoparticles can enhance mechanical properties (Cividanes et al., 2014). Also, the tensile strength of coating and bonding between steel and coating can be enhanced by using barium sulfate (Cheng et al., 2007).

Similarly, corrosion resistance of coated steel can be enhanced by increasing the cross-linking and adhesion forces (Liu et al., 2013). It was reported that the dielectric and interface properties of the coated steel rebars can be enhanced by the use of barium titanate (Cheng et al., 2007). Monetta et al. (1993) reported that the addition of about 8.5% of polyamide to epoxy could increase the density and resistance of epoxy coating from $10^6$ to $10^{11}$ $\Omega cm^2$. Similarly, Mayne (1973) reported that the use of about 10 moles per liter of $CaCl_2$ can increase the electrical resistance of the coating. The use of additives can also improve the resistance to UV degradation. For example, the use of about 2% of carbon black nanoparticles could improve the UV resistance by two times (Ghasemi-Kahrizsangi et al., 2015). The use of photostabilizers such as $TiO_2$ and ZnO are widely used additives to enhance the resistance to UV degradation (Nikafshar et al., 2017). Also, uniform distribution of such photostabilizers in the coating material is important for achieving effective and uniform UV resistance. Typically, such chemical compositions are also used for manufacturing FBE coating.

Standards such as ASTM A775 and IS 13620 specifies the following coating characteristics: coating thickness, coating continuity, coating flexibility, limitation on damage to the coating, salt spray resistance, resistance to chloride permeability, abrasion resistance, impact resistance, and resistance to cathodic disbondment. The comparison of a few specifications of two widely used standards is presented in Table 2. The review of literature and comparison of specifications of standards indicates that a few of these specifications need to be more stringent. For example, ASTM A775 specifies that the maximum amount of repaired damage should not exceed 1% of the total surface area of coated steel rebars in each

**Table 2.** Existing specifications for fusion-bonded-epoxy (FBE) coated steel rebars.

| Specification | ASTM A775 | IS 13,620 |
| --- | --- | --- |
| Maximum time to coating application after cleaning | 3 hours | 8 hours |
| Coating thickness | 177–400 μm for Rebars Number 19–57; 177–300 μm (for others) 80% < Individual measurements < 120% | 100 to 300 μm. These limits do not apply to patch area. 90% of measurements should be within limits |
| Coating continuity | ≤ 3 holidays/meter length | ≤ 6 holidays/meter length |
| Adhesion/Flexibility | No visible cracks or debonding after bending for 180° | No visible cracks or debonding after bending for 120° |
| Permissible coating damage | All damage should be repaired. Maximum allowed damage level is 1% of coating surface area | If coating damage < 4 cm$^2$, then, coating may not be required to be repaired. Maximum amount of damage should not exceed more than 2% of coating surface area |
| Storage | If circumstances require storing coated steel rebars outdoors for more than two months, protective storage measures shall be implemented to protect the material from sunlight, salt spray and weather exposure Rebars shall be covered with opaque polyethylene sheeting or other suitable opaque protective material. The covering shall be secured adequately, and allow for air circulation around the bars to minimize condensation under the covering. | No guideline |
| Coating (patch) material | Guidelines for coating material | No guideline |

0.3 m length of rebar. However, photographic evidence are available, showing the widespread use of FBE-coated steel rebars with significant damage to the coating (Kamde, 2020). These include macro-scale damage such as scratches and cracks and micro-scale damage such as pinholes and micro-cracks. Also, the quantification of such damage on coating is very challenging.

ASTM A775 recommends using the holiday detector for assessing the coating continuity that beeps when there is an electrical short circuit between the sensor and the underlying steel. The assessment of coated steel rebars using the holiday detector is time-consuming because of the small-damaged surface area and large quantity of coated steel rebars. FBE coating can shrink and crack when exposed to sunlight or UV rays (Kamde & Pillai, 2020a; Nikafshar et al., 2017). At early exposure times, the cracks may not be deep enough to get the electrical short circuit between the sensor and underlying steel. Therefore, the assessment of coating continuity using holiday detector at the manufacturing unit alone (i.e., before the possible sunlight exposure) may not be adequate. In addition, ASTM A775 recommends to repair all the visible damage at construction sites. However, there can be defects, which are not visible to naked eyes such as pinholes, UV-induced cracking, which need to be considered in the specifications. Also, the effect of repair of scratch damage at sites by repair epoxy on their electrical resistance is unknown. In short, the existing specifications need revision, which is one of the focuses of this paper.

## 1.2. Transport of moisture, oxygen and chlorides through coating

The permeability of epoxy coating is crucial to assess the corrosion performance. The absorption of water in a two-component epoxy depends on the coating composition, thickness, temperature, etc., and can be about 1 to 7% by weight of coating (Öchsner et al., 2005; Zhou & Lucas, 1999). Besides the resin, the hardener used in the coating influences the ingress of the water molecules in the polymer structure (Soles & Yee, 2000). The radius of the pores in the coating ranges from 0.2 to 0.5 nm and the radius of water molecule is about 0.13 nm. Water molecules are integrated in the polymer structure by hydrogen bridge bonds (Zhou & Lucas, 1999). The water absorption takes place in two simultaneous mechanisms (Soles & Yee, 2000); (i) via singular hydrogen bridge bonds without external energy due to low activation energy and (ii) via multiple hydrogen bridge bonds with external energy. The driving force of the transport process is the concentration gradient in the interface between the electrolyte/coating and the coating/rebar. The pore structure, temperature, and moisture affect the diffusion process since it is a non-ideal Fickian diffusion process (Zhou & Lucas, 1999) and the diffusion rate follows the Arrhenius relationship (Klopfer, 1974). Hereby, the chemical composition of the coating is of minor importance for water transport (Soles & Yee, 2000). Also, the electrical resistance between the anodic and cathodic sites has a linear relationship between ion diffusion and electrical resistance of coating, $R_C$ (Kittelberger & Elm, 1946). In general, an increase in moisture content can decrease $R_C$. Therefore, $R_C$ can be used as a performance indicator of the quality of coating and time to corrosion initiation. A good coating will have an $R_C$ higher than $10^6$ $\Omega$cm$^2$ (Bacon et al., 1948; Wang & Gao, 2016). Also, the chloride diffusion coefficient ($D_{cl, coating}$) of epoxy coating is a key performance indicator for the time to corrosion initiation (Kamde & Pillai, 2020a; Singh & Ghosh, 2005).

However, the poor handling practices and prolonged exposure to sunlight or UV rays can adversely affect $R_C$ and $D_{cl, coating}$ and result in premature corrosion (Kamde, 2020).

### 1.3. Corrosion mechanisms of FBE-coated rebars

The microclimate at the steel-coating interface influences the corrosion of FBE-coated rebars. The presence of hydrogen and oxygen in the interface between the coating and steel surface is essential to enable cathodic reaction. If only water and hydrogen are in contact with the steel without additional ions, an extended diffuse double layer can form, which prevents electrochemical reactions (Pourbaix, 1963). However, any kind of existing ions at the steel-coating interface affects the development of the electric double layer (Grundmeier et al., 2000). If aggressive ions such as chloride ions reach the interface, then anodic reactions are also possible – resulting in the corrosion initiation of steel.

The chloride threshold ($Cl_{th}$) can be defined as the minimum chloride concentration required at the steel surface to initiate corrosion. In case of FBE-coated steel rebars, chlorides have to travel through the cover concrete or mortar and then through the epoxy coating to reach the steel surface beneath. In RC structures with good quality epoxy coating (say, chloride diffusion coefficient $\approx 10^{-20}$ m$^2$/s), the time taken for chlorides to diffuse through the coating could be significant and must be considered while estimating the corrosion-free service life. However, many literature reports the chloride concentration on the coating surface at the time of corrosion initiation as the $Cl_{th}$, which is significantly higher than the $Cl_{th}$ of uncoated steel rebars (Darwin et al., 2014; Vaca 1998). Brown et al. (2006) report that the $Cl_{th}$ of FBE-coated steel rebars ranges between 0.02 and 2.3% by weight of binder. The variation in the reported $Cl_{th}$ can be due to the changes in the microclimate at the steel-coating interface. Note that the various damage or degradation to coating can result in different microclimate at the steel-coating interface (Cambier, 2014), which can alter the $Cl_{th}$ of FBE-coated steel. Note that the chloride concentration at the coating surface do not take part in corrosion of steel underneath, and can be termed as 'pseudo-$Cl_{th}$'. Therefore, it is essential to determine the $Cl_{th}$ of FBE-coated steel rebars as the chloride concentration at the steel-coating interface required to initiate corrosion (Kamde & Pillai, 2020a, 2020b). The $Cl_{th}$ determined in this manner and the $D_{Cl, concrete}$ and $D_{Cl, coating}$ must be considered to estimate the service life of RC systems with FBE-coated steel rebars. This paper highlights the importance of including such performance indicators in the standards and guidelines.

It can be summarized that the resistance to corrosion of FBE-coated steel rebars depends on the ingress of moisture, oxygen, and chlorides through the coating and their continued availability to sustain the corrosion reactions. Also, the corrosion propagation of FBE-coated rebars is usually governed by crevice or under-film corrosion mechanisms and the propagation period can be considered as less than 5 years (Pianca et al., 2005; Sagüés et al., 2010a; Weyers et al., 1998).

## 2. Research Significance

Worldwide, fusion-bonded-epoxy (FBE) coated steel rebars are used in anticipation of enhanced corrosion resistance. However, in many construction projects and the results in this paper show that the inadequate quality of coating, rough handling and sunlight or UV exposure of FBE-coated rebars at sites can lead to scratches and microcracks of epoxy coating, which in turn can lead to premature corrosion. Also, the currently adopted specifications are inadequate to ensure desired corrosion resistance of FBE-coated rebars in concrete. The recommendations on the making the specifications more stringent and additional performance indicators presented in this paper can be incorporated in ASTM A775 and will help engineers to evaluate the properties of FBE coating and FBE-coated steels in a better way and ensure the desired corrosion resistance and service life.

## 3. Experimental program

Table 3 summarises the test program adopted for Phase 1 and Phase 2 of this study. Phase 1 involves the assessment of coating characteristics, which can influence the performance of FBE coating and are provided in the existing specifications. Phase 2 involves studies on performance indicators of FBE coating or coated steel rebars, which can be included in the specifications to help to achieve desired service life.

### 3.1. Phase 1: characteristics of FBE coating, as per existing specifications

#### 3.1.1. Thickness, continuity, and flexibility of FBE coating

FBE-coated steel rebars from 10 lots were used for this. The 8 mm diameter rebars were cut to a length of 150 mm, with continuous application of coolant oil. Then, the thickness of epoxy coating on the 150 mm long rebar specimens were measured non-destructively; using an electromagnetic coating thickness gauge. A total of 20 measurements were taken at the central 100 mm length of the

**Table 3.** Test variable and number of specimens.

| Property of FBE coating/FBE coated steel rebar | Type of specimen | Measurement technique/ test method | No. of Specimens |
|---|---|---|---|
| Coating thickness | 150 mm long coated steel rebars | Electromagnetic coating thickness gauge | 10 |
| Coating continuity | Coating steel rebars | Holiday detector | 10 |
| | Peeled-off coating samples | SE micrographs | 30 |
| | UV exposed peeled-off coating samples | | |
| Coating flexibility | 90° bent coated steel rebars | Visual Observation (VOB) | 10 |
| Permissible damage | Lollipop specimens with FBEC-ND, FBEC-SD, and FBEC-UV | EIS | 15 |
| Chemical compositions | Peeled-off coating samples | EDX analysis | 45 |
| Resistance to degradation due to exposure to UV rays | Peeled-off coating samples | SE micrographs | 15 |
| Resistance of coating | Coated steel plates | EIS, LA-ICP-MS | 25 |
| Resistance of coating to moisture and ionic transport | Coated plates and peeled-off coatings | LA-ICP-MS, NMR | 25 |
| Chloride threshold | lollipop specimens with uncoated, FBEC-ND, FBEC-SD, and FBEC-UV coated steel rebars | EIS and chemical analysis as per SHRP 330 | 20 |
| Diffusion coefficients | Peeled off coating from coated steel rebars after initiation of corrosion was detected | EDX analysis | 10 |

specimens. Note that all these measurements were taken at locations between the ribs and at the top of the transverse ribs.

These specimens were then visually inspected by naked eyes for discontinuities and then the holidays were recorded using a holiday detector. Five specimens were exposed to ultraviolet (UV) rays in accelerated weathering chamber for 10 days, which is equivalent to about one month of UV exposure to natural sunlight in Chennai, India during Summer with an average UV index of 10. Then, 5 × 5 mm size samples of the coating were peeled-off from all the ten specimens. Micrographs of these samples were obtained using the scanning electron (SE) microscope, and the effects on coating continuity were evaluated.

Coating flexibility tests were performed on ten 500 mm long specimens of 8 mm diameter FBE coated steel rebars. As recommended in ASTM A775, the rebars were bent to an angle of 90 degrees and then visually assessed for cracking and debondment or peeling of coating.

### 3.1.2. Effect of damaged, degraded, and repaired epoxy coating on corrosion characteristics

To assess the effect of the damage or degradation of the coating and the repair or recoating of damaged epoxy coating (as usually done at construction sites) on the corrosion characteristics, FBE-coated steel rebars were cut to 110 mm long pieces – using an abrasive cutter and with continuous application of coolant oil. Twenty such pieces were prepared – four sets of five pieces with different damage type, see Figure 1 for photographs. Five pieces were used in as-received conditions and denoted as FBEC-ND (indicating 'No known Damage' case). The



(a) FBE coated steel with no damage

(b) FBE coated steel with scratch damage to the coating

(c) FBE coated steel with repaired scratch damage

**Figure 1.** FBE coated steel with different coating conditions.

coating on another five pieces were damaged (at the centre of each rib on both sides) by scratching the rib surfaces using a grit paper and denoted as FBEC-SD (indicating 'Scratch Damage'). The coating on another five pieces were scratched in similar manner and then repaired (or cold-bonded) with a layer of a two-component epoxy and denoted as FBEC-RSD (indicating 'Repaired Scratch Damage'). A fourth set of five pieces were kept in an artificial weathering chamber and exposed to UV rays for 10 days as per ASTM G154 (2016) and denoted as FBEC-UV. All these 20 FBE-coated rebar pieces were used for preparing the lollipop specimens for corrosion studies (see Figure 2). Twenty lollipop specimens were cast and cured
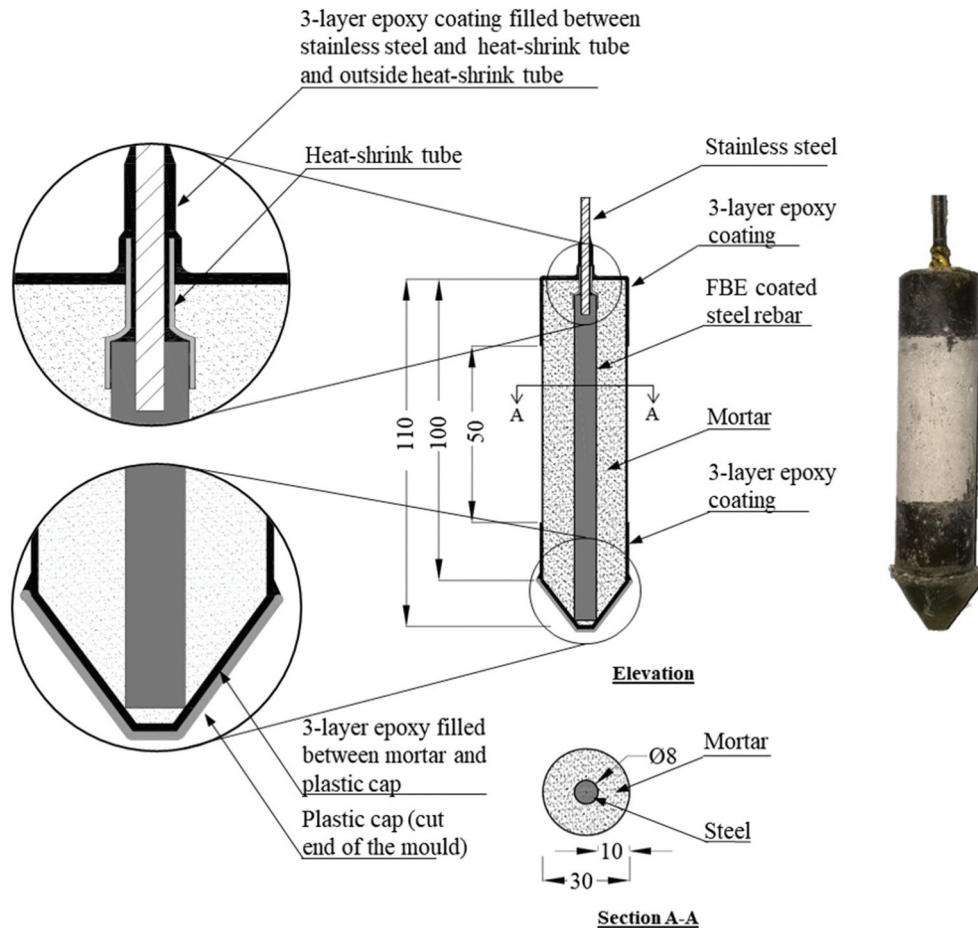
**Figure 2.** Schematic and photograph of lollipop specimen used for electrochemical testing (Kamde, 2020).

for 28 days. Then, EIS responses were obtained from these lollipop specimens after saturating them in sodium chloride solution for 2 days. The Nyquist and Bode plots were analyzed and the effect of the various damage types on the corrosion characteristics of FBE-coated steel rebars were assessed. The same specimens (five of FBEC-ND, FBEC-RSD, and FBEC-UV cases) were also used to evaluate the electrical resistance of FBE coating ($R_C$) with these coating conditions and embedded in cementitious environment. Later, $R_C$ is proposed to be included as a performance indicator of FBE coating or coated steel rebars.

### 3.2. Phase 2: additional characteristics of FBE coating and FBE-coated steel rebars

#### 3.2.1. Chemical composition and UV-resistance
The chemical composition of FBE coating was obtained by using the area Energy Dispersion X-ray (EDX) analysis. For this, three $5 \times 5$ mm size samples of coating were peeled-off from 15 FBE-coated steel rebar pieces. Thereby, a total of 45 coating samples were used for the EDX analysis. During EDX analysis, electron beams

with an energy of 20 keV (at a working distance of $\approx$ 10 mm) were used and the following elements were detected during the analysis: Ba, S, O, N, Ti, Zn, Ca, Fe and Cl.

To investigate the UV-resistance of coating, the time of initiation of cracks on FBE coating were studied. For this, a total of 18 coating samples were peeled off from rebars, glued to a foam tape, and exposed to UV rays (with a wavelength of 340 nm) in the accelerated weathering chamber, designed as per ASTM G154 (2016). Figure 3(a) shows the photographs of the process to peeled-off coating specimen. Figure 3(b) shows the 18 coating samples peeled off and ready for UV exposure. Three coating samples were removed from the weathering chamber at 1, 3, 5, 7, 10, and 12 days of exposure and SE micrographs were obtained at a magnification of 20,000X. The time to initiation of cracks in each specimen was recorded.

#### 3.2.2. Resistance to chloride ingress through coating
This investigation had focussed on the diffusion behaviour of chlorine and iodine. The coating was exposed
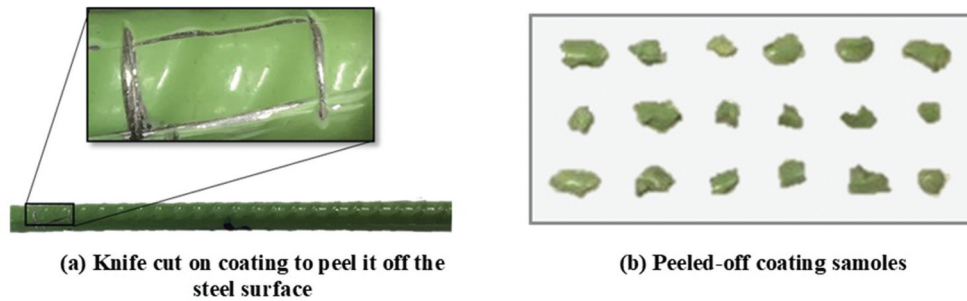
(a) Knife cut on coating to peel it off the steel surface

(b) Peeled-off coating samoles

**Figure 3.** Coating samples peeled off from FBE coated steel rebars and ready for UV exposure.

to different chlorine and iodine solutions, and the depth and time-dependent ion transport was characterized via laser ablation inductively coupled plasma mass spectrometry (LA-ICP-MS). The purpose of the LA-ICP-MS measurements was to evaluate the depth-dependent ingress of ions in the epoxy coating. During this test, the spray system converts the test solution to an aerosol, which is later ionized through an inductively couple plasma (argon) at 5,000–10,000°C. A quadrupole ion deflector isolates the unnecessary photons and neutrons from the ion beam. Next, a quadrupole mass separates the ions according to their mass and charge, followed by ion acceleration in direction to the detector. The aim is to bring the ions to the ion optic through an interface, which connects the mass filter with the mass spectrometry. The detector counts every incoming ion, and the resulting signal is expressed by counts per second (cps). The detection limit of the ICP-MS is regardless of the mass in the order of a few µg/g up to ng/l. Elements with higher ionization potential such as the halogens have poorer detection limits since fewer ions are generated in the plasma.

Here, in contrast to a pure ICP-MS, which analyzes a test solution, the material under investigation is locally vaporized through a laser, and the resulting solid aerosol is analyzed. The laser unit consists of a laser with a wavelength of 213 nm and a pulse interval of 3 to 5 nos (NWR213 der Firma 'New Wave'). The diameter of the laser beam (3 to 110 µm) determines the mass of the vaporized material. Higher signal intensities lead to lower detection limits (Garcia et al., 2008). The laser frequency is in the range of 5 to 20 Hz. Consequently, the combination of laser diameter, laser frequency, and laser energy level determines the ablation depth. Ablation of spots and lines are possible. The advantage of the line ablation is that ion profiles can be generated several times through the ablation of the same line. Additionally, a line scan leads to a greater volume of the tested material and consequently, the number of signals per second is high.

The high intrinsic chlorine content of epoxy coating and the high detection limit of chlorides demand an alternative analysis. The diffusion of iodide completes the investigation due to following reasons: Iodide shows same transport characteristics due to comparable atomic radii and iodides are not a constituent part of the source material; iodine has a lower ionization potential and with 127 u, a higher atomic mass than chlorine (35 u), it is easily detectable with the mass spectroscopy; iodides are an ideal transport indicator. To investigate the diffusion of ion, coating films have been peeled off from the coated steel plates. In general, only defect-free coating material is used in this investigation, as checked using a holiday detector.

### 3.2.3. Chloride diffusion coefficient of FBE coating with and without defects

To determine the effect of prolonged exposure to sunlight and its effect on the chloride diffusion coefficient ($D_{cl, coating}$) of epoxy coating, five lollipop specimens, as shown in Figure 2, were cast using FBEC-ND and FBEC-UV rebars. The lollipop specimens were subjected to cyclic wet-dry exposure using simulated concrete pore solution with chlorides until the initiation of corrosion was detected. This was done by identifying a statistically significant increase in the corrosion rate or inverse polarisation resistance of the steel-coating interface ($1/R_{P, S-C}$); using a procedure outlined in Kamde and Pillai (2020a). After the initiation of corrosion was detected, the chloride concentrations at various depths of coating (i.e., 0, 50, 100, 150, 200, 250, 300 µm) were obtained using the EDX technique. To avoid cross-contamination of chlorides from various depths in the cross-section of the epoxy coating, the exposed rebars were half-cut using an abrasive cutter. Then, the remaining half of the rebar (including the coating portion under evaluation) was bent and fractured along the half-cut plane. Using this procedure, three chloride profiles each from five coating samples were obtained. These chloride profiles and Fick's second law of

diffusion was used to determine the $D_{cl, coating}$ of FBE coating before and after UV exposure.

### 3.2.4. Chloride threshold of steel-coating interface

To determine the $Cl_{th}$, five lollipop specimens (see Figure 2) each with following steel rebars were cast: (i) uncoated (UC), (ii) FBEC-ND, (iii) FBEC-SD, and (iv) FBEC-UV. A three-electrode corrosion cell was used for EIS tests. In this, the embedded steel rebar was the working electrode, nickel-chromium mesh placed circumferentially to the lollipop specimen was the counter electrode; and saturated calomel electrode was the reference electrode. See Kamde (2020) for details. The simulated concrete pore solution (0.03% Ca(OH)$_2$ + 2.23% KOH + 1.04% NaOH + 96.6% of distilled water) with 3.5% NaCl was used as the immersion solution. Following input parameters were used for the EIS tests: the alternating current potential amplitude of ± 10 mV, a frequency range from $10^6$ Hz to 0.01 Hz, the direct current potential was maintained at the measured half-cell potential, and 10 data points per decades were collected. The signal response was analyzed and resistances offered by each layer (mortar, coating, steel-coating interface) were quantified using the Equivalent Electrical Circuit (EEC), which is presented in Kamde (2020). Then, the change in $R_{P, S-C}$ with respect to the exposure time was monitored. The corrosion was defined to initiate when a statistically significant increase in the inverse $R_{P, S-C}$ was observed; detected using the statistical procedure outlined in Kamde and Pillai (2020a).

Upon initiation of corrosion, a mortar of 0.5 mm depth adjacent to uncoated and coated steel was powdered and collected. The chloride concentration in the powdered mortar was determined using the guidelines prescribed in (SHRP-S-330, 1993). For specimens with uncoated steel rebars, this chloride concentration was defined as the $Cl_{th}$. However, for specimens with FBE-coated steels, the chlorides at the coating-mortar interface do not participate in the corrosion activities of the underlying steel, hence the chloride concentration at the coating-mortar interface is defined as Pseudo-$Cl_{th}$. The chloride concentration beneath the coating (i.e., at the steel-coating interface) takes part in the corrosion process and is defined as the $Cl_{th}$ of the FBE-coated steel rebars (Trejo, 2020).

To determine the chloride concentration at steel-coating interface, Energy Dispersion X-ray analysis (EDX) was done on the inside surface of the peeled-off FBE coating (i.e. at the steel-coating interface). The average of three measurements is defined as the $Cl_{th}$ of each FBE-coated steel rebar (in % by weight of the coating). Then, these measurements were converted to

% by weight of binder (%bwob) – by assuming that the chloride concentrations in the coating surface and the mortar surface in contact are similar – and defined as the $Cl_{th}$ of FBE-coated steel rebars.

## 4. Results and discussions

### 4.1. Phase 1: characteristics of FBE coating, as per existing specifications

#### 4.1.1. Coating thickness ($t_{coating}$)

Figure 4(a) shows the variation of $t_{coating}$ on the rebars from each lot. The dash lines corresponding to LLI and LLA – representing the lower limits of $t_{coating}$ prescribed by IS 13,620 (2015) and ASTM A 775/A 775M – 17 (2017), respectively. The dash-dot-dash line corresponding to UL represents the identical upper limit of $t_{coating}$ specified by both IS 13,620 (2015) and ASTM A 775/A 775M – 17 (2017). The markers in Figure 4(a) represents the $t_{coating}$ measured on the FBE-coated steel rebars at locations between two ribs and on top of the ribs; and was
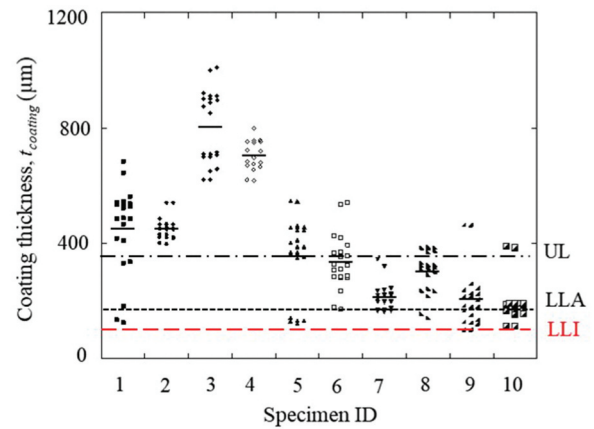


(a) Variation of coating thickness
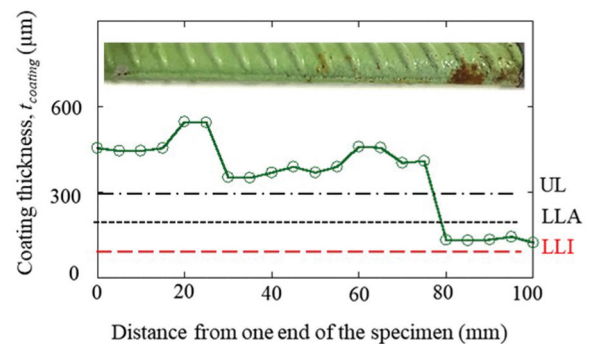


(b) Evidence of initiation of corrosion at the location with $t_{coating}$ < 175 μm

**Figure 4.** Variation of coating thickness and evidence of corrosion activities at locations with $t_{coating}$ < 175 μm in commercially available FBE coated steel rebars [LLI: lower limit of $t_{coating}$ as per IS 13,620 (2015); LLA: lower limit of $t_{coating}$ as per ASTM A775; UL: upper limit of $t_{coating}$ as per IS 13,620 (2015) and ASTM A775].

found to range from about 100 to 1000 μm. Figure 4(b) shows the photograph of a typical 100 mm long FBE-coated steel rebar extracted from a typical lollipop specimen. This was intentionally exposed to chloride solution for 4 weeks after the initiation of corrosion. Figure 4(b) shows that the locations with $t_{coating}$ < 175 μm experiences early corrosion. This indicates the importance of ensuring the minimum $t_{coating}$ of 175 μm throughout the rebar (ASTM A 775/A 775M – 17, 2017; FHRA, 1976; Kobayashi & Takewaka, 1984; Manning, 1996). However, IS 13,620 (2015) recommends a minimum $t_{coating}$ of 100 μm, which needs to be modified. Also, $t_{coating}$ was found to be more than the upper limits specified in the standards, which can result in a reduction in bond strength between steel and concrete (Kobayashi & Takewaka, 1984; Miller et al., 2003). Miller et al. (2003) also reported that the bond strength is not significantly affected until the $t_{coating}$ is more than 420 μm. The ASTM A775 states, 'the average of all recorded coating thickness measurements shall not be less than the specified minimum thickness or more than the specified maximum thickness'. The current study recommends to replace this statement with '*No single recorded coating thickness shall be less than 175 μm or more than 350 μm.*' Also, the coating measurement is an easy, quick, and non-destructive quality check that can be done upon arrival

of rebars at construction sites. Hence, the recommendation of ASTM A 775/A 775M – 17 (2017) for a minimum of 10 recorded $t_{coating}$ measurements per rebar must be followed strictly.

### 4.1.2. Coating continuity (number of holidays or pinholes)

FBE-coated steel rebar specimens were visually inspected and no damage or cracks were observed; see the first photograph and first micrograph (at 300X) in Figure 5(a). However, an inspection using a holiday detector indicated many holidays in the coating of the same specimens; see second micrograph (at 5000X) in Figure 5(a). These holidays are of about 10 μm diameter, which are not visible to the naked eyes. Then, additional specimens were exposed to sunlight for 12 days in UV chamber (see ASTM G154), which is equivalent to 1 month of sunlight in Chennai, India with an average UV index of 10 during summer (Kamde & Pillai, 2020a). The specimens were visually inspected and no cracks were observed with naked eyes. However, the first micrograph (from the same specimen; at 300X) in Figure 5 (b) shows that the FBE coating can undergo UV-degradation resulting in new pinholes (see black regions or dots on the surface of epoxy coating)
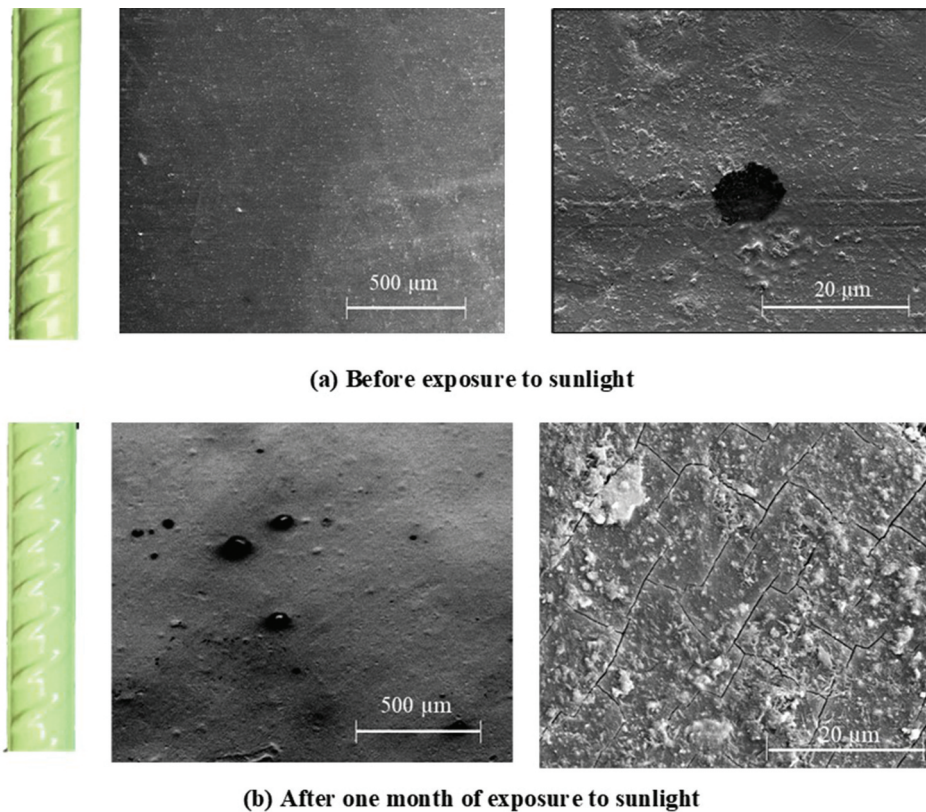


(a) Before exposure to sunlight



(b) After one month of exposure to sunlight

**Figure 5.** Effect of exposure to sunlight/UV on FBE coating (obtained from same rebar lot).

with diameter ranging up to 100 μm. The appearance of new pinholes in large number can be attributed to the evaporation of volatile materials in the coating; indicating inadequate chemical composition of coating material. In addition, UV rays or sunlight exposure also led to microcracks, which are due to restrained shrinkage of coating, see second micrograph (at 5000X) in Figure 5(b). This is mainly an effect of inadequate polymer structure and composition. Therefore, visual inspection alone is inadequate and the authors recommend to measure the number of pinholes or cracks or scratches at the manufacturing plant and at construction site; in particular, just before the placement of concrete around the rebars. Such approach will force the builders to handle the rebars with care to avoid abrasion-induced scratching and to prevent the prolonged exposure to sunlight or UV (even after the rebar cages are in place).

### 4.1.3. Coating flexibility

ASTM A775 and IS 12,620 recommend testing the coating flexibility by bending to 180 and 120 degrees, respectively. Among the ten specimens tested, the coating in all the specimens were cracked and disbonded from steel surface even when the bend angle reached 90 degrees (see Figure 6) – indicating inferior quality of FBE coating. Therefore, to achieve the desired quality, the epoxy coating materials and processes need to be standardized. Also, as suggested by ASTM A 775/A 775M – 07B (2007), the FBE-coated steel rebars should be coated only after bending. However, providing the guidelines for flexibility test using bending operations in Table 1 of ASTM A 775/A 775M – 07B (2007) can misguide the practitioners. Therefore, a note should be added to Table 1 of ASTM A775 with the text 'This table is provided only to check the flexibility of FBE
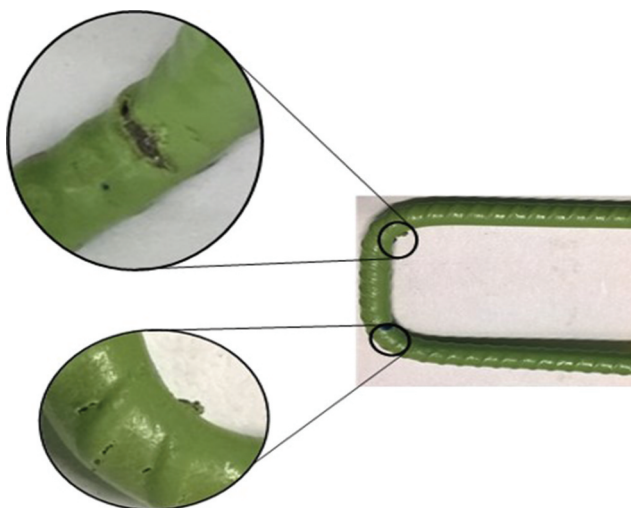


**Figure 6.** Damage to FBE coating due to 90° bending.

coating. To meet structural detailing requirements, the rebars should be bent prior to the application of coating. Bending of rebars after the application of coating is not recommended.'

### 4.2. Phase 2: additional characteristics of FBE coating and FBE-coated steel rebars

#### 4.2.1. Chemical composition and UV resistance

Figure 7 shows that the variation of concentrations of elements such as C, Ba, S, Cl, Ca, Fe, Ti, Zn, etc. were found to be significantly high – indicating that the elements are not distributed uniformly in the coating. Such non-uniformity can affect the pore structure, shrinkage resistance, corrosion resistance, and mechanical properties of FBE-coated steel rebar systems (Monetta et al., 1993; Wang et al., 2008). Figure 8 shows the scanning electron micrographs obtained from the surfaces of epoxy coating samples at 0 and 10 days of exposure in UV chamber. No cracks were found in the FBEC-ND samples, see Figure 8(a). FBEC-UV coating samples after exposure to UV rays for about 10 days showed significant microcracks, see Figure 8(b) with micrograph at 20,000X. The photostabilizers (i.e. $TiO_2$ and ZnO) could prevent disintegration or microcracking of the coating until 10 days of exposure in UV chamber. EDX analysis on epoxy coating surfaces revealed that the cracking of epoxy coating was initiated, where the photostabilizers (ZnO or $TiO_2$) were deficient or not available. It was also found that the epoxy coating did not crack, where the concentration of Ti and Zn was more than 5 and 2% by weight of the coating, respectively. Therefore, it is recommended to include appropriate ranges on photostabilizers and/or UV-induced crack resistance in ASTM A775 and other relevant standards or guidelines. The total duration of exposure to sunlight (from manufacturing to embedment in concrete) should be restricted to less than one month to avoid microcracking, which could reduce the corrosion resistance of the rebars.

#### 4.2.2. Electrical and water-uptake resistance of coating

Figure 9(a) shows that the weight of all plates was found to be increasing with increased exposure time. At the beginning of the experiment, the water uptake is very steep. Then, it slows down with the prolonged exposure of plates to the electrolyte. The overall water uptake of the plates in contact to concrete after around 150 days is about 1.1 wt.%, which may not be the saturation limit. The water uptake in the coating when coated plates are
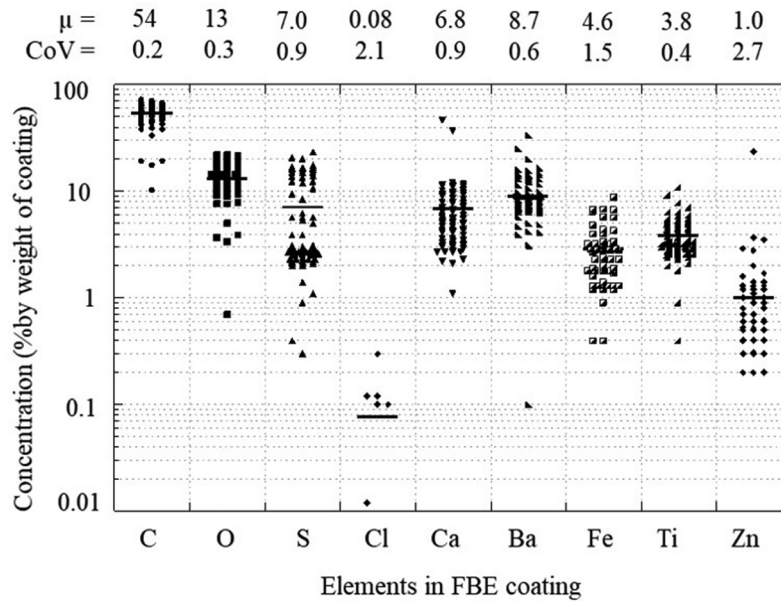
**Figure 7.** Variation in chemical composition of FBE coating.



(a) FBEC-ND coating without cracks
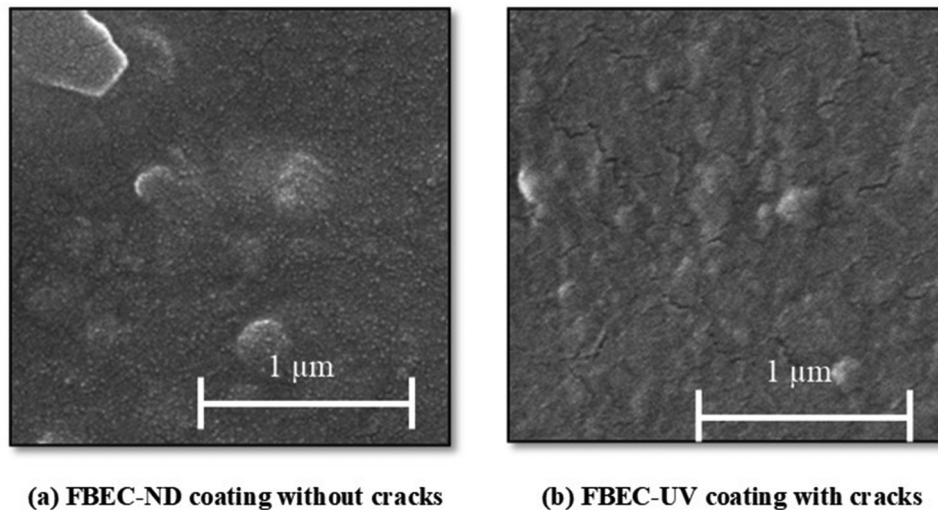
(b) FBEC-UV coating with cracks

**Figure 8.** Cracking of FBE coating due to exposure to sunlight/UV rays.

directly exposed to the electrolyte was found to be 1.4 wt.%, which is 20% higher than that in concrete. Also, the plates in the concrete with higher water-to-binder ratio show slightly higher water-uptake. In contrast, the cement type has no pronounced influence in the water uptake. Figure 9(b) shows that with an increase in water uptake, the resistance of coating ($R_C$) decreases. After the exposure period of 150 days, the average $R_C$ of coated plates embedded in the concrete and exposed to solution is about 3.1 to 4.1 $\times 10^7$ $\Omega$m; whereas the average $R_C$ of coated plates directly exposed to the solution is 2.9 $\times 10^7$ $\Omega$m.

The objective of the NMR-measurement is to determine the water ingress profiles in the coating by determination of the amplitudes (NMR-signal) in each layer (0, 100, 200, 300, 400, 500, 600 μm). Figure 10(a) and (c) show the amplitude of the free induction decay of the excited hydrogen isotopes. Initially, the 90° pulse is generated transversal to the magnetization. The 180° pulse follows after a certain delay leading to the detection of the first spin echo after the echo time. Here, the echo time is 0.076 ms (spin echo 1.216 ms) in each layer, and the signal length contains 16 echoes in total. The summation of each echo in each layer leads to a characteristic value, see Figure 10(a) and (c), and corresponds to a qualitative moisture profile. The area integral of the amplitudes was assumed to be the total moisture content in the coating. Then, the moisture
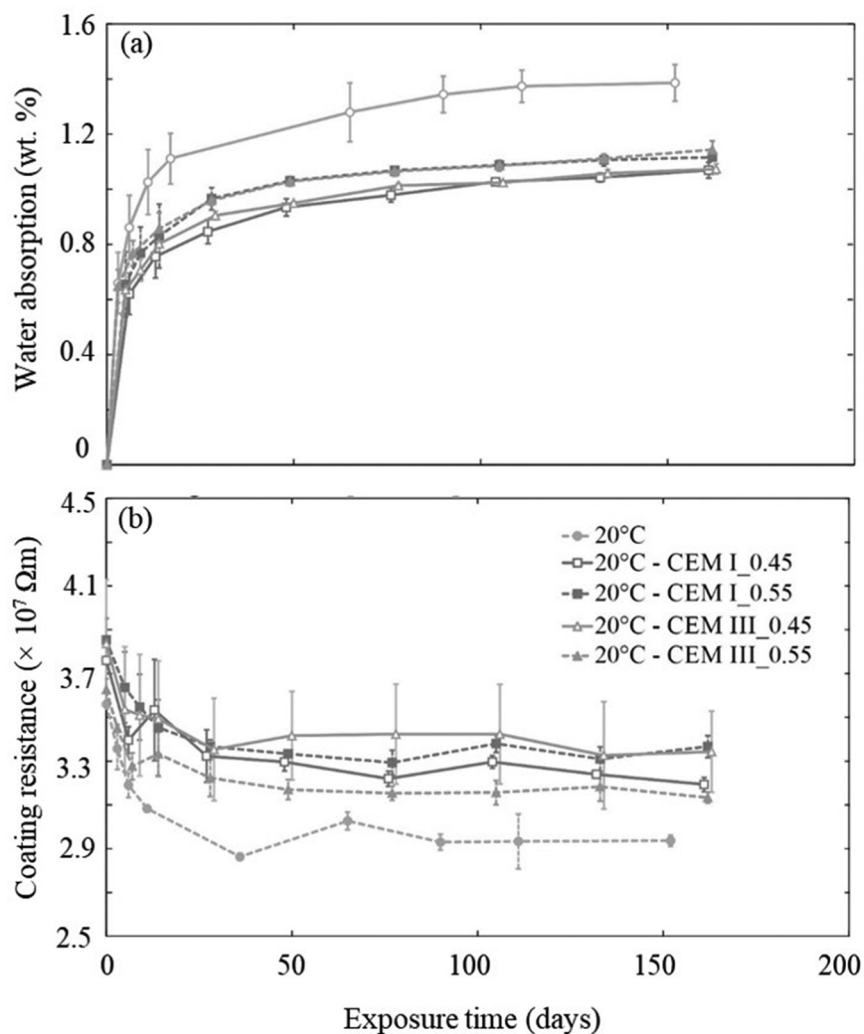
**Figure 9.** Water absorption of epoxy-coated plates exposed to concrete and solution: (a) time-dependent water absorption; (b) time-dependent coating resistance.

increase can be proportionally assigned to each layer. The bar diagram [Figure 10(b) and (d)] shows the quantitative moisture profiles. Figure 10(b) shows the moisture profiles for plates exposed in concrete with portland cement and the water-to-binder ratio of 0.45 and 0.55. The first measurement, '0 d' corresponds to the state before the plates have been exposed to an electrolyte.

All qualitative moisture gradients of the reference measurements '0 d' show a profile from the exposed side to the coating/metal interface. These profiles can be regarded as the initial moisture condition. The corresponding thermogravimetric analysis of the same material results in the moisture content of 0.2 wt.%. The decrease of the moisture content from the air (exposed) side to the metal side is in line with the results of the pore structure of the coating. It is assumed that at the beginning of the exposure, the pores are filled with

gas. Since the existence of excitable hydrogen nuclei affects the intensity of the NMR signal, it can be concluded that an increasing porosity leads to low signal levels. After the exposure, the single-sided NMR measurement can detect the water uptake with respect to the depth. The highest water uptake is on the exposure side of the coating. After 7 days, the water content in the first layer of 100 μm reaches values of about 0.4 wt.%, which is twice the initial moisture content. The moisture content in the coating layer in the vicinity of the steel is in the range of the intrinsic moisture condition of about 0.66 wt.%. Consequently, the conclusion is that the water can penetrate through polymer and thus through epoxy coating.

As per ASTM A775, the coating thickness shall be in the range of 175 to 300 μm. Here, the investigated coatings are thicker than recommended coating thickness. Thus, based on these results, a complete moisture
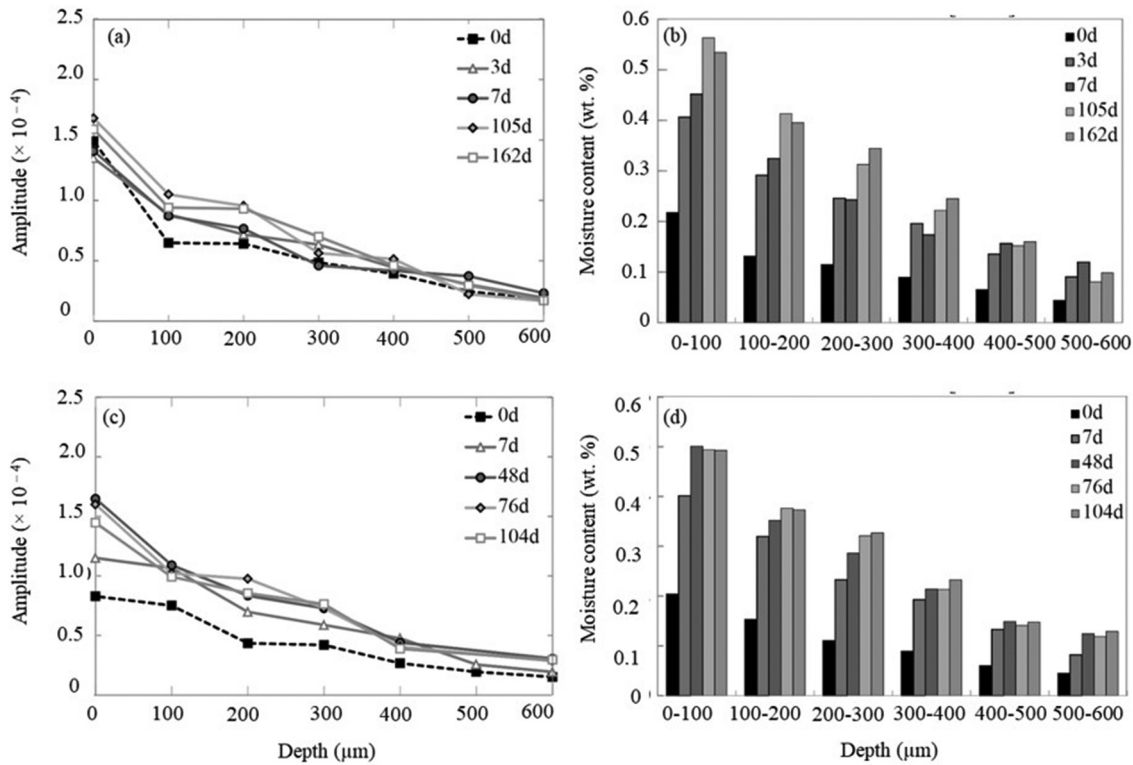
**Figure 10.** Time-dependent moisture profiles based on NMR-results (a) epoxy coated plate in Portland cement concrete (w/b = 0.55) – summation of the echoes at different times, (b) calculated time dependent quantitative moisture profile, (c) epoxy-coated plate in Portland cement concrete (w/b = 0.45) summation of the echoes at different times, (d) Calculated time dependent quantitative moisture update.

penetration is possible in ordinary epoxy coating on rebars. Under the submerged condition, the moisture content increases close to the coating–steel interface after about 1 week. The NMR results show as well that the moisture content in the submerged samples is 20% greater than in the coated specimens embedded in concrete systems and immersed in the electrolyte. If the moisture content in epoxy is high enough to enable water penetration in the coating–steel interface, corrosion cannot be excluded.

Figure 11 shows that the electrical resistance, $R_C$, of FBE coating without damage or degradation is greater than $10^6$ $\Omega cm^2$. The $R_C$ is dependent on the thickness of coating, $t_{coating}$, and a typical epoxy coating with $t_{coating}$ of 600 μm can have an $R_C$ of about $10^{11}$ $\Omega cm^2$. Therefore, $R_C$ should be measured on coated steel with recommended $t_{coating}$. Wang and Gao (2016) reported that the $R_C > 10^8$ $\Omega.cm^2$ indicates a good quality of the coating. Similarly, Kessler et al. (2016) reported that an undamaged FBE coating in a 24-year-old bridge had an $R_C$ of $\approx 10^8$ $\Omega cm^2$, and could provide corrosion protection to the underneath steel rebars. In this case, the FBEC rebars were handled very delicately and no damage or cracks on the coating were allowed (say, similar to FBEC-ND case) – hence, good performance is expected. On the
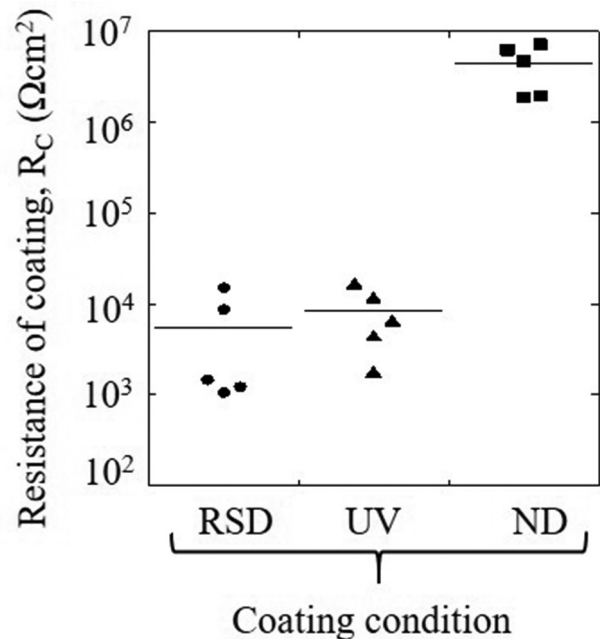


**Figure 11.** Effect of inadequate construction practices on the resistance of coating.

other hand, the $R_C$ offered by FBEC-RSD and FBEC-UV coatings was about $10^3$ and $10^4$ $\Omega cm^2$, respectively,

which is about 3 or 4 orders less than the $R_C$ of FBEC-ND coating. Therefore, it can be concluded that inadequate practices such as exposure to sunlight (with UV index > 8) and repaired coating at construction sites cannot offer the required $R_C$ and protection against corrosion.

### 4.2.3. Resistance to chloride ingress through coating

First, the results of the reference series exposed to deionized water serve to estimate the noise and the basic signal caused by the coating itself. It is assumed that the deionized water contains nearly no sodium, chloride, and iodide ions. The elements of interest are sodium (Na 23), chlorine (Cl 35), and iodine (I 127). The analysis of the ablated material from the coating detects a very few sodiums and no iodine. This result is in agreement with the assumption that the deionized water does not contain sodium or iodide. In contrast, the intensity of the chlorine signal is very high since epichlorohydrin is one of the parts of this polymer. Figure 12(b) shows that the chlorine signal oscillates around a constant value ($1.0 \times 10^3$ cps, counts/s) over the whole depth of the coating. This high basic chloride value confirms that it is not possible to detect any penetration of free chloride ions in the coating.

Figure 12 summarizes the analyses of the coatings exposed to sodium iodide solution. Here, the elements of interest are sodium, chlorine, and iodine. In both series, the chlorine signal oscillates around a high value compared to the reference results [Figure 12(b)]. The value is significantly high that any ingress of chloride can not be evaluated. The sodium signal in both series shows a similar profile. Close to the boundary zone, the sodium signal increases over time up to a value of $3.0 \times 10^5$ cps. There is ingress of sodium, which has an opposite charge than chloride or iodide. However, the sodium penetration is only detectable within the time frame up to a depth of around 4 μm. Figure 12(c) shows that the Iodides could also penetrate to a depth of 4 μm in the coating [see detail plot in Figure 12(c)], which is in agreement with penetration of sodium. It represents that the elements, sodium and iodine, penetrate in parallel. Assuming that an epoxy coating is in line with the standard and has a coating thickness of about 175 μm it would take 33 years until the iodine would reach the steel surface. This value emphasizes the barrier effect of epoxy coating with regard to aggressive agents such as chlorides. However, the quality of the coating gets reduced during the prolonged exposure to sunlight; a quantification of the chloride ingress rate in such cases is discussed next.

### 4.2.4. Chloride diffusion coefficient of FBE coating

It is very common to see exposure of FBE-coated rebars to sunlight (even for about five to 6-months due to prolonged
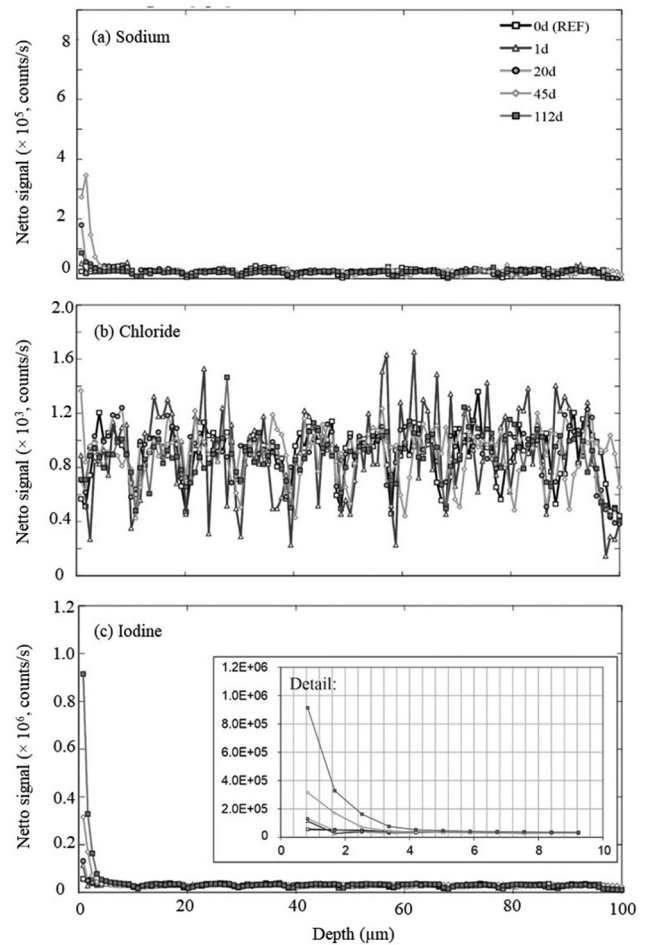


**Figure 12.** Results of the depth-dependent element concentration of coatings exposed to 10 m.-% sodium iodide with LA-ICP-MS: sodium (Na23), chlorine (Cl35) and iodine (I127); the detail highlights the iodine profile in the first 10 μm of the coating.

storage and delay in construction stages). Figure 13 shows that the diffusion coefficients of FBE coating ($D_{cl, coating}$) can increase from $1.6 \times 10^{-20}$ m²/sec to $8.7 \times 10^{-18}$ m²/sec with a 10-day exposure in UV chamber (equivalent to about 1 month of sunlight exposure). This is an increase by two orders of magnitude and indicates faster penetration of chlorides due to UV-induced microcracks in the coating and significant reduction in the time to initiation of corrosion. Therefore, $D_{cl, coating}$ is a key performance indicator to be included in the standards and guidelines and needed for service life estimation.

### 4.2.5. Chloride threshold of steel-coating interface ($Cl_{th}$)

Figure 14 shows that the $Cl_{th}$ of FBE-coated steel rebars without and with damage or degradation are less than that of uncoated steel rebars. The average chloride concentrations on the coating surface (say, coating-mortar interface) at the time of initiation of corrosion in FBEC-
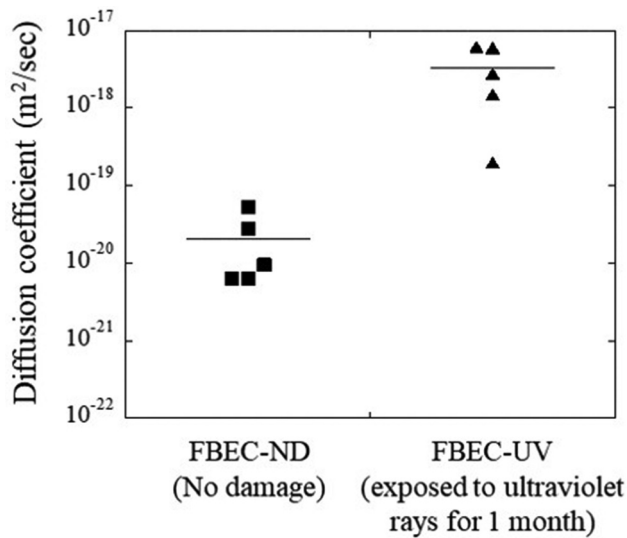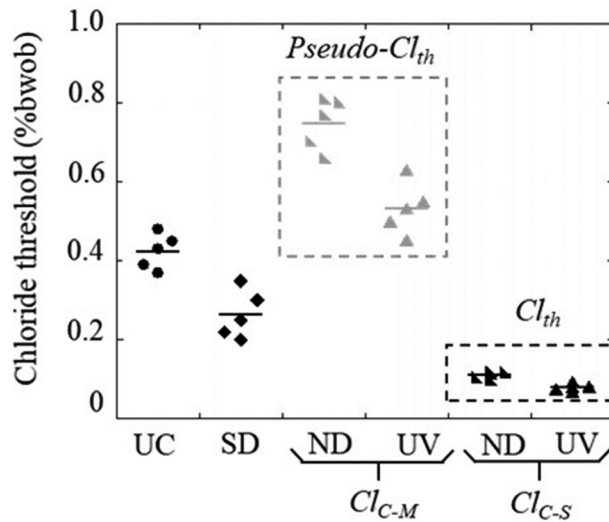
**Figure 13.** Diffusion coefficients of FBE coating.



Notes: %bwob: % by weight of binder; $Cl_{th}$ : chloride threshold; $Cl_{C-M}$ : chloride concentration at coating mortar interface; ND: no damage; SD: scratched damage.

**Figure 14.** Chloride threshold determined using the cs-ACT test method.

ND and FBEC-UV specimens were 0.75 and 0.53% by weight of the binder (%bwob) – a 1/3$^{rd}$ reduction. However, these chlorides at the coating surface do not participate in corrosion process. Therefore, they are not the true $Cl_{th}$ of FBE-coated steel rebars and are termed as *pseudo-$Cl_{th}$*. Then, the chloride concentration at the inner face of the coating (i.e. at the steel-coating interface) was determined using EDX, and the average $Cl_{th}$ for FBEC-ND and FBEC-UV specimens was found to be 0.12 and 0.07%bwob, respectively – about 40%

reduction due to UV exposure. The difference in the $Cl_{th}$ of FBEC-ND and FBEC-UV type steel rebars is attributed to differences in the microclimate at the steel-coating interface – say, available pH, moisture, oxygen, and chlorides; and is in agreement with the findings in (Ann & Song, 2007; Cambier et al., 2014; Hansson et al., 2000; Pianca et al., 2005).

In the case of FBEC-SD specimens, steel surface at the scratch or crack locations are in direct contact with the chloride-contaminated mortar. Hence, the corrosion initiation is not governed by the slow diffusion process through the coating. Hence, the $Cl_{th}$ in this case was determined as the chloride concentration at the coating-mortar interface and was found to be 0.22% bwob, which is higher than the FBEC-ND and FBEC-UV. However, this higher $Cl_{th}$ of FBEC-SD rebars does not really help in enhancing the service life because of the direct access to chlorides at the scratch or crack locations in epoxy coating. Note that the $Cl_{th}$ is also dependent on the defect size in the epoxy coating and other physicochemical conditions surrounding to the metal surface (Angst et al., 2009; Kessler et al., 2016). The $Cl_{th}$ of FBE-coated steel rebars can change based on the surface damage conditions of the coating. Therefore, the authors recommend determining the $Cl_{th}$ on the test specimens that reflect the surface damage conditions of the FBE-coated rebars used in the field and then use the $Cl_{th}$ determined in this way for service life estimation.

## 5. Recommended specifications

This paper recommends a few additional performance indicators and modifications for the existing specifications in ASTM A775 to help achieve the desired performance of FBE-coated steel rebars in concrete. Table 4 summarises the proposed specifications on coating characteristics such as coating thickness, the concentration of photostabilizers (Ti and Zn), coating continuity, flexibility of coating, and permissible damage level. Also, directions on the additional performance indicators such as electrical resistance of epoxy coating, resistance to water uptake, chloride threshold of the steel-coating interface ($Cl_{th}$) and chloride diffusion coefficients of coating ($D_{cl,\ coating}$) and their use in estimating service life are provided in Table 4. It is anticipated that these modifications will help to prevent the use of FBE-coated rebars with inferior quality. It must be noted that the paper does not intend to prevent the use good quality FBE-coated rebars.

## 6. Conclusions

ASTM A775 is the most developed standard for controlling the performance of fusion-bonded-epoxy (FBE)

**Table 4.** Specifications for fusion-bonded-epoxy (FBE) coated steel rebars.

| Parameter or factor | Existing specification in ASTM A775 | Proposed specification |
|---|---|---|
| Coating thickness | 'No single recorded … shall be less than 80% … ' | 'No single recorded coating thickness measurement shall be less than 175 μm or more than 1.2 times the specified maximum coating thickness' |
| Coating continuity | Suggests "… to determine the acceptability of the steel reinforcing bars prior to shipment. | Suggests '… to determine the acceptability of the steel reinforcing bars prior to shipment and prior to embedding in the concrete.' |
| Resistance to UV degradation | Not provided | No crack should appear on coating surfaces (at magnification of 20,000X) after equivalent exposure time. |
| Exposure to sunlight | ' … to less than two months.' | 'Exposure of FBE coated steel rebars to sunlight must be minimized to a total duration of less than one month. No crack/damage to coating should be visible on surface micrographs taken at $20,000 \times$ magnification.' |
| Flexibility of coating | Table 1 of ASTM A 775/A 775M – 07B (2007) | Note to Table 1 in ASTM A775 "*This table is provided only to check the flexibility of FBE coating. To meet structural detailing requirements, the rebars should be bent prior to the application of coating. Bending of rebars after the application of coating is not recommended.*" |
| Resistance of FBE coating and patching material ($R_C$) | Not provided | $R_C > 1 \times 10^6$ $\Omega cm^2$ |
| Service life | Not provided | '$Cl_{th}$ of FBE coated steel rebars is the chloride concentration at the steel-coating interface that is required to initiate corrosion and must be determined. If the rebar is exposed to sunlight for more than 30 days, then the $Cl_{th}$ needs to be assumed as 50% of that of the FBE coated steel with pristine coating. The chloride diffusion coeficient of coating ($D_{cl, coating}$) significantly affects the corrosion initiation time. Both $Cl_{th}$ and $D_{cl, coating}$ must be determined on specimens reflecting field conditions and used for service life estimation.' |

coated steel rebars. However, inadequate manufacturing and construction site practices, and premature corrosion are widespread, which is seeking further comprehensive and stringent specifications. Also, many agencies have either banned or recommended not to use FBE-coated steel rebars. This paper presents results on various characteristics of epoxy coating and suggests modifications to the standards to enhance the corrosion resistance of FBE-coated steels. It is concluded that adequate and uniform coating thickness, uniform distribution of photostabilizers, and limiting the exposure to sunlight to a maximum of 1 month are important to ensure to achieve the desired corrosion resistance. Also, bending of rebars must be done prior to the application of coating and the coated rebars must be carefully handled to avoid abrasion-induced scratch damage. Inadequate coating characteristics and handling during transportation and storage at sites can lead to faster degradation of coating and early initiation of corrosion even at low chloride levels. In addition, the following performance indicators were found to be dominating in ensuring the desired performance of FBE coating: (i) electrical resistance of the coating ($R_C$), (ii) resistance to water uptake, (iii) chloride thresholds of the steel–coating interface ($Cl_{th}$), (iii) chloride diffusion coefficient of coating ($D_{cl, coating}$). It was found that a high $R_C$ of epoxy coating was a good indicator of its performance in resisting the ingress of moisture or water and chlorides. Also, the $Cl_{th}$ and $D_{cl, coating}$ of FBE-coated steel-concrete systems, is found to vary significantly due to abrasion or scratching at sites and exposed to sunlight for longer than 1 month. Hence, such tests must be done on rebar specimens reflecting the true field conditions and the expected deviations in $Cl_{th}$ and $D_{cl, coating}$ must be accounted for estimating their service life. This paper provides a set of stringent specifications to be incorporated in the existing standards (say, ASTM A775) and other guidelines.

## Abbreviations

| | |
|---|---|
| %bwob | : % by weight of binder |
| Clc-s, $Cl_{th}$ | : Critical chloride threshold of steel-coating interface |
| $t_{coating}$ | : Coating thickness |
| $D_{cl, concrete}$ | : Chloride diffusion coefficient of concrete |
| $D_{cl, coating}$ | : Chloride diffusion coefficient of coating |
| EIS | : Electrochemical impedance spectroscopy |
| EEC | : Equivalent Electrical Circuit |
| FBE | : Fusion-Bonded-Epoxy |
| FBEC-ND | : FBE-coated steel rebars in as-received condition with no damage or degradation |
| FBEC-RSD | : FBE-coated steel rebars with repaired scratch damage |
| FBEC-SD | : FBE-coated steel rebars with scratch damage |
| FBEC-UV | : FBE-coated steel rebars after 10 days of exposure to UV rays |
| LA-ICP-MS | : Laser ablation inductively coupled plasma mass spectrometry |
| NMR | : Nuclear magnetic resonance |
| RC | : Reinforced concrete |
| $R_C$ | : Resistance of the coating |
| $R_{P, C-S}$ | : Polarization resistance of the coating-steel interface |
| RSD | : Repair scratch damage |
| SD | : Scratch damage |
| S-C | : Steel-Coating interface |
| SEM | : Scanning electron microscope |

UC     : Uncoated
UV     : Ultraviolet

## Data availability statement

The authors confirm that the data supporting the findings of this study are available within the article.

## Disclosure statement

No potential conflict of interest was reported by the authors.

## Notes on contributors

*Deepak K. Kamde* earned his B.Tech. degree in Civil Engineering from SRCOEM, Nagpur and M. Tech. degree in Structural Engineering from SVNIT Surat, Gujarat. In 2020, he earned a Ph.D. degree in Civil Engineering from IIT Madras. He is Project Officer at IITM, Chennai, India. His research interests include corrosion, durability, service life estimation, repair, and cathodic protection of concrete structures. Email: deepak.kamde89@gmail.com

*Marc Zintel* holds a Diploma and Ph.D. degree in Civil Engineering from Technical University of Munich, Germany. He is Business Development Manager of Construction Products at Swiss Steel AG, Emmenbrücke, Switzerland. His research interests include durability of reinforced concrete structures, life cycle costs and corresponding sustainability approaches. Email: mzintel@swiss-steel.com

*Sylvia Kessler* holds a Diploma from RWTH Aachen University, Germany and Ph.D. degree in Civil Engineering from Technical University of Munich, Germany. She is a Full Professor of Engineering Materials and Building Preservation at Helmut-Schmidt-University / University of the Federal Armed Forces Hamburg, Germany. Her research interests include durability, service life prediction, non-destructive testing and maintenance and repair of reinforced concrete structures. Email: sylvia.kessler@hsu-hh.de

*Radhakrishna G. Pillai* holds M.S. and Ph.D. degree in Civil Engineering from Texas A&M University, USA. He is an Associate Professor in the Department of Civil Engineering, Indian Institute of Technology Madras, India. His research interests include corrosion, durability and service life estimation of steel-cementitious systems, maintenance/repair, and cathodic protection of concrete structures. Email: pillai@iitm.ac.in

## ORCID

Deepak K. Kamde  http://orcid.org/0000-0003-1794-5695
Sylvia Kessler  http://orcid.org/0000-0002-1335-1104
Radhakrishna G. Pillai  http://orcid.org/0000-0003-3672-8768

## References

Angst, U., Elsener, B., Larsen, C. K., & Vennesland, O. (2009). Critical chloride content in reinforced concrete — A review. *Cement and Concrete Research*, *39*(12), 1122–1138. doi:10.1016/j.cemconres.2009.08.006

Ann, K. Y., & Song, H. W. (2007). Chloride threshold level for corrosion of steel in concrete. *Corrosion Science*, *49*(11), 4113–4133. doi:10.1016/j.corsci.2007.05.007

ASTM A 775/A 775M – 07B. (2017). *Standard specification for epoxy-coated steel reinforcing bars*. American Society for Testing and Materials, West Conshohocken, PA 19428-2959. United States.

ASTM G154. (2016). *Standard Practice for Operating Fluorescent Ultraviolet (UV) Lamp Apparatus for Exposure of Nonmetallic Materials*. American Society of Testing and Materials, West Conshohocken, PA 19428-2959. United States.

Bacon, C. R., Smith, J. J., & Rugg, F. M. (1948). Electrolytic Resistance in Evaluating Protective Merit of Coatings on Metals. *Journal of Industrial & Engineering Chemistry*, *40*(1), 161–167. doi:10.1021/ie50457a041

Bahadori, A. (2015). Engineering Guidelines for Protective Coatings in Buried and Submerged Steel Structures. *Essentials of Coating, Painting, and Lining for the Oil, Gas and Petrochemical Industries*, 411–439. Gulf Professional Publishing. doi:10.1016/B978-0-12-801407-3.00006-7

Brown, M. C., Weyers, R. E., & Sprinkel, M. M. (2006). Service life extension of virginia bridge decks afforded by epoxy-coated reinforcement. *Journal of ASTM International*, *3*(2), 1–13. doi:10.1520/JAI11793

Cambier, S. M. (2014). "Atmospheric corrosion of coated steel; relationship between laboratory and field testing." Ph.D. Thesis, Ohio State University, The Ohio State University.

Cambier, S. M., Posner, R., & Frankel, G. S. (2014). Coating and interface degradation of coated steel, Part 1: Field exposure. *Electrochimica acta*, *133*, 30–39. Elsevier Ltd. doi:10.1016/j.electacta.2014.04.004.

Cheng, K. C., Lin, C. M., Wang, S. F., Lin, S. T., & Yang, C. F. (2007). Dielectric properties of epoxy resin-barium titanate

composites at high frequency. *Materials Letters*, *61*(3), 757–760. doi:10.1016/j.matlet.2006.05.061

Cividanes, L. S., Simonetti, E. A. N., Moraes, M. B., Fernandes, F. W., Thim, G. P., & Tecnol, I. (2014). Influence of Carbon Nanotubes on Epoxy Resin Cure Reaction Using Different Techniques : A Comprehensive Review. *Polymer Engineering and Science*, *54*(11), 2461–2469. doi:10.1002/pen.23775

Darwin, D., O'Reilly, M., Browning, J., Locke, C. E., Virmani, Y. P., Ji, J., Gong, L., Guo, G., Draper, J., & Xing, L. (2014). Multiple Corrosion-Protection 35 Systems for Reinforced-Concrete Bridge Components: Laboratory Tests. *Journals of Materials in Civil Engineering*, *26*(36), 1–9. doi:10.1061/(ASCE)MT.1943-5533.0000991

FHRA. (1976). Interim Report No. 2 - NEEP No. 16 Coated Reinforcing Steel for Bridges. Washington D.C.

Garcia, C., Lindner, H., & Niemax, K. (2008). Laser ablation inductively coupled plasma mass spectrometry - current shortcomings, practical suggestions for improving performance, and experiments to guide future development. *Journal of Analytical Atomic Spectrometry*, *24*(1), 14–26. doi:10.1039/B813124B

Ghasemi-Kahrizsangi, A., Shariatpanahi, H., Neshati, J., & Akbarinezhad, E. (2015). Degradation of modified carbon black/epoxy nanocomposite coatings under ultraviolet exposure. *Applied Surface Science*, *353*, 530–539. Elsevier B.V.. doi:10.1016/j.apsusc.2015.06.029.

Griffith, A., & Laylor, H. M. (1999). *Epoxy Coated Reinforcement Study*. Oregon: Oregon Department of Transportation Research.

Grundmeier, G., Schmidt, W., & Stratmann, M. (2000). Corrosion protection by organic coatings: Electrochemical mechanism and novel methods of investigation. *Electrochimica acta*, *45*(15–16), 2515–2533. doi:10.1016/S0013-4686(00)00348-0

Hansson, C. M., Haas, R., Green, R., Evers, R. C., Gepraegs, O. K., & Al-Assar, R. (2000). *Final Report, Corrosion Protection Strategies for Ministry Bridges*. University of Waterloo.

Kamde, D. K. (2020). *Electrochemical, bond, and service life parameters of coated steel - cementitious systems exposed to chlorides*. Indian Institute of Technology Madras, Chennai.

Kamde, D. K., & Pillai, R. G. (2020a). *Effect of sunlight/ultraviolet exposure on the corrosion of fusion bonded-epoxy (FBE) coated steel rebars in concrete*pp. 843-859. Corrosion (Houston). doi:10.5006/3588

Kamde, D. K., & Pillai, R. G. (2020b). "Chloride-induced corrosion of Fusion-Bonded-Epoxy coated steel rebars in concrete and its effects on service life." (Unpublished work)

Kessler, S., Angst, U., Zintel, M., & Gehlen, C. (2016). Defects in epoxy coated reinforcement and its impact on service-life of concrete structures. *Fib Structural Journal*, *16*(3), 398–405.

Kittelberger, W. W., & Elm, A. C. (1946). Water Immersion Testing of Metal Protective Paints: Role of Osmosis in Water Absorption and Blistering. *Journal of Industrial & Engineering Chemistry*, *38*(7), 695–699. doi:10.1021/ie50439a015

Klopfer, H. (1974). *Wassertransport durch Diffusion in Feststoffen insbesondere Baustoffen, Kunststoffen, Beschichtungen*. Wiesbaden, Germany: Bauverlag GmbH. ISBN: 3762503834.

Kobayashi, K., & Takewaka, K. (1984). Experimental studies on epoxy coated reinforcing steel for corrosion protection. *International Journal of Cement Composites and Lightweight Concrete*, *6*(2), 99–116. doi:10.1016/0262-5075(84)90039-3

Liu, B., Fang, Z. G., H. Bin, W., & Wang, T. (2013). Effect of cross linking degree and adhesion force on the anti-corrosion performance of epoxy coatings under simulated deep sea environment. *Progress in Organic Coatings*, *76*(12), 1814–1818. Elsevier B.V.. doi:10.1016/j.porgcoat.2013.05.022.

Manning, D. G. (1996). Corrosion performance of epoxy-coated reinforcing steel: North American experience. *Construction and Building Materials*, *10*(5), 349–365. doi:10.1016/0950-0618(95)00028-3

Mayne, J. E. O. (1973). The mechanism of the protection of iron and steel by paint, Anti Corros. (October) 3–8.

Miller, G. G., Kepler, J. L., & Darwin, D. (2003). Effect of epoxy coating thickness on bond strength of reinforcing bars. *ACI Structural Journal*, *100*(3), 314–320.

Monetta, T., Bellucci, F., Nicodemo, L., & Nicolais, L. (1993). Protective properties of epoxy-based organic coatings on mild steel. *Progress in Organic Coatings*, *21*(4), 353–369. doi:10.1016/0033-0655(93)80050-K

Nikafshar, S., Zabihi, O., Ahmadi, M., Mirmohseni, A., Taseidifar, M., & Naebe, M. (2017). The effects of UV light on the chemical and mechanical properties of a transparent epoxy-diamine system in the presence of an organic UV absorber. *Materials*, *10*(2), 1–18. doi:10.3390/ma10020180

Öchsner, W. P., Bergk, B., Fischer, E., & Gaszner, K. (2005). Wasseraufnahme von Beschichtungen: Sorptionsisothermen für Wasser in organischen Beschichtungen und deren Einfluss auf die Beschichtungseigenschaften. *Farbe und Lack*, *111*, 42–51.

Pianca, F., Schell, H., & Cautillo, G. (2005). The performance of epoxy coated reinforcement : Experience of the Ontario ministry of transportation. *International Journal Materials and Product Technology*, *23*(3/4), 286–308. doi:10.1504/IJMPT.2005.007732

Pourbaix, M., "Atlas d'équilibres électrochimiques," Centre Belge d'Etude de la Corrosion CEBELCOR (Paris, France: Gauthier- Villars & Cie., 1963).

Pyć, W. A., Weyers, R. E., Weyers, M., Mokarem, D. W., & Zemajtis, J. (2000). *Field performance of epoxy-coated reinforcing steel in virginia bridge decks*. Charlottesville, Virginia: Virginia Department of Transportation.

Sagüés, A. A., Lau, K., & Accardi, A. Final Report "Mechanistic Issues on Corrosion Performance of Dual Polymer–Zinc Coated Rebar", Gerdau-Ameristeel, 2010a

Sagüés, A. A., Lau, K., Powers, R. G., & Kessler, R. J. (2010b). Corrosion of epoxy-coated rebar in marine bridges - A 30 year perspective. *CORROSION*, *66*(6), 065001. doi:10.5006/1.3452397

Sagüés, A. A., Perez-Duran, H., & Powers, R. (1991). Corrosion performance of epoxy-coated reinforcing steel in marine substructure service. *Corrosion*, *47*(11), 884. doi:10.5006/1.3585202

Sagüés, A. A., & Zayed, A. M. (1991). Low-Frequency Electrochemical Impedance for Measuring Corrosion of Epoxy-Coated Reinforcing Steel in Concrete. *Corrosion*, *47*(11), 852–859. doi:10.5006/1.3585197

Sánchez, A. N., & Sagüés, A. A. (2013) Potential-Dependent Chloride Threshold in Reinforced Concrete Damage

Prediction – Effect of Activation Zone Size. NACE, paper No. 2704.

Shi, X., Nguyen, T. A., Suo, Z., Liu, Y., & Avci, R. (2009). Effect of nanoparticles on the anticorrosion and mechanical properties of epoxy coating. *Surface & Coatings Technology*, *204*(3), 237–245. Elsevier B.V.. doi:10.1016/j.surfcoat.2009.06.048.

SHRP-S-330. (1993). "Standard Test Method for Chloride Content in Concrete Using the Specific Ion Probe." Strategic Highway Research Program, National Research Council, Washington, DC.

Singh, D. D. N., & Ghosh, R. (2005). Unexpected deterioration of fusion-bonded epoxy-coated rebars embedded in chloride-contaminated concrete environments. *Corrosion*, *61*(8), 815–829. doi:10.5006/1.3278216

Smith J. L., Virmani Y. P. (1996). *Performance of Epoxy-Coated Rebars in Bridge Decks*, Federal Highway Administration Research and Technology, Washington D.C. https://www.fhwa.dot.gov/publications/publicroads/96fall/p96au6.cfm.

Soles, C. L., & Yee, A. F. (2000). A discussion of the molecular mechanisms of moisture transport in epoxy resins. *Journal of Polymer Science. Part B, Polymer Physics*, *38*(5), 792–802. doi:10.1002/(SICI)1099-0488(20000301)38:5<792::AID-POLB16>3.0.CO;2-H

Trejo, D. (2020). *Personal discussion with Prof. David Trejo*. Chennai: Oregon State University.

Vaca, E.C. (1998). Corrosion Performance of Epoxy-Coated Reinforcement in Aggressive Environments, Ph.D. Thesis, University of Texas at Austin.

Wang, X. H., & Gao, Y. (2016). Corrosion behavior of epoxy-coated reinforced bars in RC test specimens subjected to pre-exposure loading and wetting-drying cycles. *Construction and Building Materials*, *119*, 185–205. Elsevier Ltd. doi:10.1016/j.conbuildmat.2016.05.066.

Wang, Z., Zhang, F., Song, N., & Ni, L. (2008). The Influence of Barium Sulfate on the Mechanical Properties of Glass/Epoxy Resin Composite. *Polymers & Polymer Composites*, *16*(4), 257–262. doi:10.1177/096739110801600405

Weyers, R. E., Pyc, W., & Sprinkel, M. M. (1998). Estimating the service life of epoxy-coated reinforcing steel. *ACI Materials Journal*, *95*(5), 546–557.

Zhou, J., & Lucas, J. P. (1999). Hygrothermal effects of epoxy resin. Part I: The nature of water in epoxy. *Polymer*, *40*(20), 5505–5512. doi:10.1016/S0032-3861(98)00790-3